Pathology - Research and Practice 215 (2019) 152591

Contents lists available at ScienceDirect

Pathology - Research and Practice

journal homepage: www.elsevier.com/locate/prp

miR-433 suppresses tumor progression via Smad2 in non-small cell lung cancer

Jianing Li[a], Meng Chen[b], Baiquan Yu[a,*]

[a] Department of Respiratory, The Second Affiliated Hospital of Harbin Medical University, China
[b] Department of Respiratory, The Fourth Affiliated Hospital of Harbin Medical University, China

ARTICLE INFO

Keywords:
miR-433
Smad2
Smad signaling
Non-small cell lung cancer

ABSTRACT

The role of transforming growth factor beta (TGF-β) in lung cancer is well known. TGF-β-mediated cellular proliferation and angiogenesis through similar to mothers against decapentaplegic homolog 2 (Smad2) protein has also been well elucidated. Smad2 is a predicted target for a microRNAs, namely miR-433. microRNAs are a significant class of non-coding RNAs which play an important role in epigenetic regulation. Here, we show that miR-433 directly binds to Smad2, which is shown to be upregulated in non-small cell lung carcinomas (NSCLC). miR-433 expression is downregulated in NSCLC tissues and cells. Overexpression of miR-433 is associated with decreased expression of proteins - namely Cyclin D1, MMP-2/TIMP-2, and MMP-9, and consequently reduced cell proliferation and invasion phenotypes. Complementation of miR-433 leads to rescue of these disrupted phenotypes. miR-433 mediates its action via Smad2 and Id-1. miR-433 may be a candidate worth further exploration for its prognostic and therapeutic potential in NSCLC.

1. Introduction

China faces an increasing burden of cancer, with the total number of cases being higher than the global average. Among the different cancers in China, non-small cell lung carcinomas (NSCLC) contribute significantly to the country's cancer burden, as well as that of the world [2]. Lifestyle and environmental changes are known contributors to this increasing disease burden. However, metastasis and invasiveness are major attributes that are responsible for the poor prognosis of NSCLC [1].

A number of aberrant pathways associated with NSCLC have been studied using high throughput approaches. Unsurprisingly, the dysregulated pathways impact cellular metabolism and the regulation of the cell cycle and DNA damage. Dysregulation of even one pathway may seemingly affect other pathways, as each of these are inter-connected and orchestrate cellular events. Thus, aberration of these pathways leads to cellular proliferation, by inhibition of apoptosis and induction of angiogenesis, thereby facilitating cancer metastasis [11,21,22].

One such pathway commonly studied in lung cancer and other cancers is the transforming growth factor beta (TGF-β) pathway [8,18]. The TGF-β pathway is involved in several biological processes including cellular growth, proliferation, programmed cell death and extra cellular matrix remodeling. TGF-β and other proteins of the TGF superfamily have a bi-modal functionality. Whilst they are protective in early stage tumors by restricting tumor growth, they promote tumor cell proliferation in later stages. These contrasting effects are mediated through similar to mothers against decapentaplegic (Smad) proteins [12,24]. Smad proteins regulate the expression of several genes.

While TGF superfamily-mediated [25] activation of Smad has been well documented, epigenetic modification of endogenous Smad and subsequent alteration of TGF-mediated activation has received very little attention [17]. One such mechanism of epigenetic modification occurs through the action of microRNAs, such as miR-433. miR-433 has been studied for its role in human tumorigenesis and growth, and its dysregulation has been associated with gastric carcinoma [19], breast cancer [27], and hepatocellular carcinoma [26]. A recent study also identified a role of miR-433 in NSCLC. However, its molecular targets and underlying mechanisms have remained less explored and therefore elusive to date.

Through a bioinformatics-based approach (Targetscan), we identified Smad2 as a potential target of miR-433. Binding of miR-433 at both its 3′ and 5′ ends led us to hypothesize that miR-433 may have a potential role in the regulation of lung cancers through alteration of the Smad signaling pathway. We first proved that miR-433 profile was altered in lung tumors in comparison to the normal tissues. Additionally, through *in vitro* models we have shown that over-expression of miR-433-3p and miR-433-5p led to a reduction in the endogenous expression of Smad2. We also show that this reduced expression is a

* Corresponding author at: Department of Respiratory, The Second Affiliated Hospital of Harbin Medical University, 246 Xuefu Road, Harbin 150086, China.
E-mail address: hydhxkyu@163.com (B. Yu).

https://doi.org/10.1016/j.prp.2019.152591
Received 22 April 2019; Received in revised form 17 July 2019; Accepted 9 August 2019

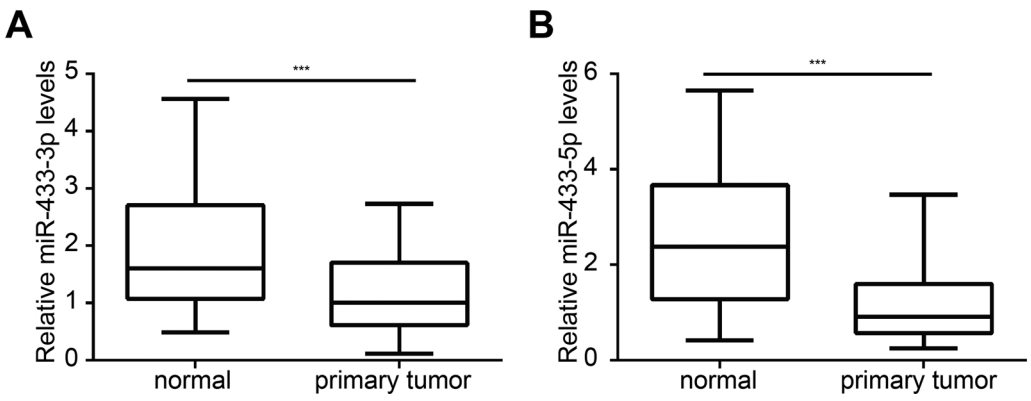

Fig. 1. *miR-433* expression is decreased in NSCLC. (A) The expression levels of *miR-433-3p* were determined in primary NSCLC tissues and normal adjacent tissues by qRT-PCR. ***$P <$ 0.001 vs. normal group. (B) The expression levels of *miR-433-5p* were determined in primary NSCLC tissues and normal adjacent tissues by qRT-PCR. ***$P <$ 0.001 vs. normal group.

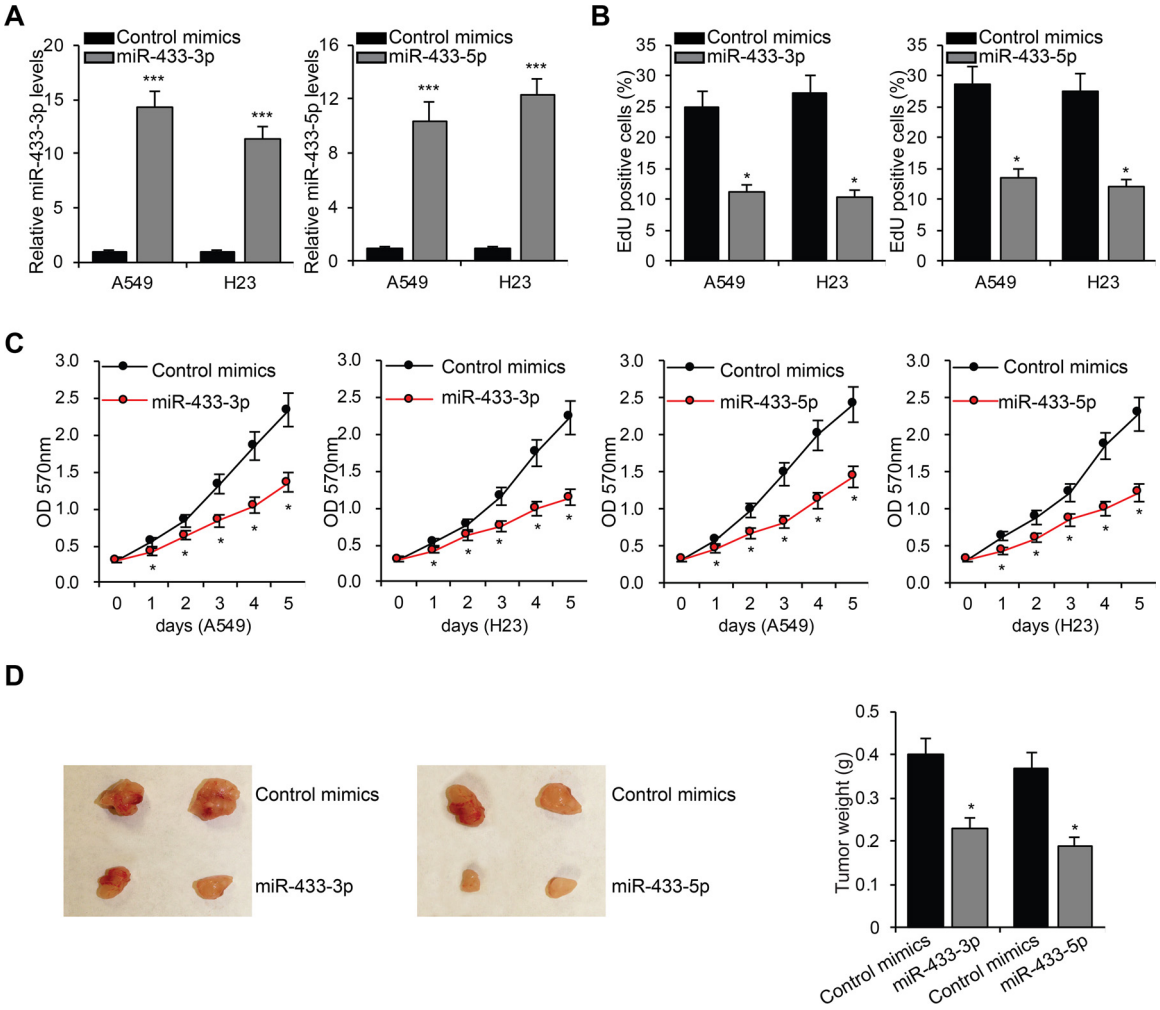

Fig. 2. *miR-433* reduces A549 and H23 NSCLC cell proliferation. (A) qRT-PCR analysis of *miR-433-3p* and *miR-433-5p* expression in A549 and H23 cells transfected with *miR-433* mimic or control miRNA mimic. (B) EdU assay of A549 and H23 cells transfected with *miR-433* mimic or control miRNA mimic. (C) MTT assay analysis of cell proliferation of A549 and H23 cells transfected with miR-433 or control miRNA mimic. (D) The nude mice were subcutaneously injected with A549 cells of LV-Control mimics or LV-*miR-433* for 25 days. Tumor weight was examined in each group. *$P <$ 0.05, ***$P <$ 0.001 vs. control mimics group.

consequence of direct targeting of Smad2 by miR-433 for which a fusion construct of the 3′-Untranslated Regions (3′-UTR) sequence of Smad2 coupled to *Renilla* luciferase was employed. We further explored the influence of miR-433 on cellular proliferation and invasion and also identified the plausible molecular pathways for these processes. Our results are suggestive of a role for miR-433 in the regulation of the Smad pathway with consequences for cellular proliferation and tumorigenesis.

2. Materials and methods

2.1. Tumor specimen collection

The study was undertaken at the Department of Respiration, second affiliated hospital of the Harbin Medical University. Fifty patients reporting to the department between 2013 and 2018 were recruited for the study. The subjects were recruited upon a confirmed diagnosis of NSCLC. Fifty such patients with diagnostic confirmation and without a

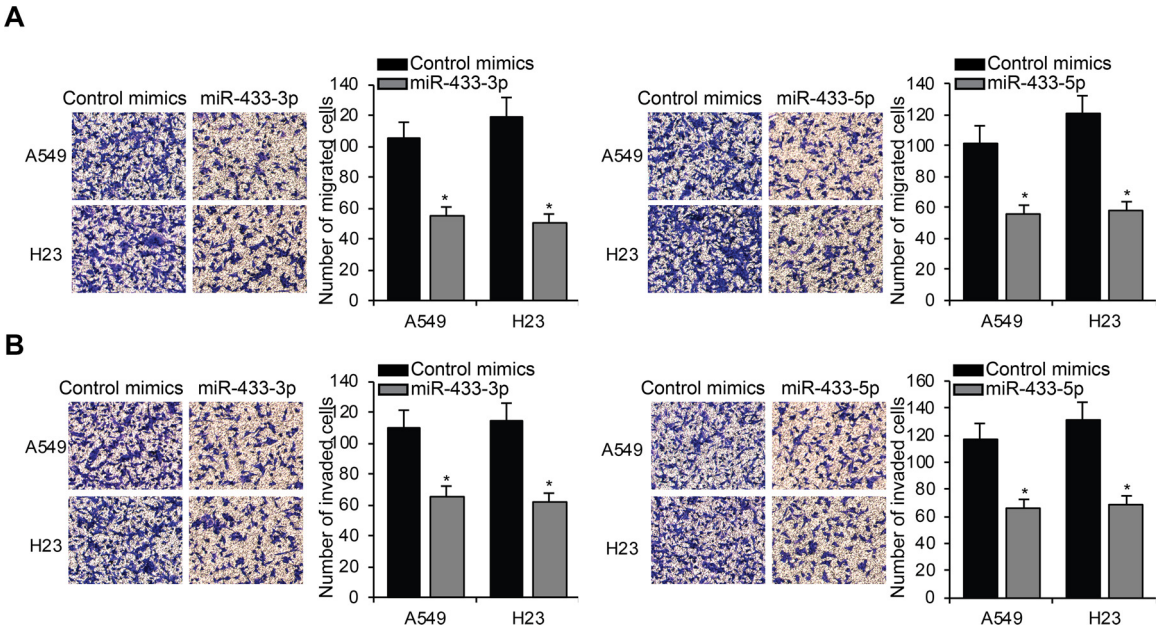

Fig. 3. *miR-433* inhibits A549 and H23 NSCLC migration and invasion. A549 and H23 cells were transfected with control miRNA or miR-433. Cell migration (A) and invasion (B) were investigated using transwell assays. Counts of invasive and migrated cells are shown (×50 magnification). *$P <$ 0.05 vs. control mimic groups.

history of anti-carcinoma therapy and/or surgical resection for lung cancers were included for this study. The clinicopathological characteristics of NSCLC patients are listed in Supplemental Table 1. Through a written informed consent, subjects were recruited for a surgical excision of the NSCLC samples and paired adjacent normal tissue. The samples were snap frozen in liquid nitrogen to be preserved at −80 °C until further analysis. All experimental protocols were performed in accordance with the Declaration of Helsinki and approved by the Research Ethics Committee of the Second Affiliated Hospital of Harbin Medical University.

2.2. Cell culture

NSCLC cell lines A549, H23, H1869 and H1650 were obtained from the American Type Culture Collection (ATCC, Manassas, VA, USA). As per the instructions of the repository, Dulbecco's modified Eagle's medium (DMEM) (#11965118, Invitrogen, Carlsbad, USA) supplemented with 10% fetal bovine serum (#16140, FBS; Invitrogen) were used for cell maintenance and culture. Antibiotics (100 U/ml penicillin, and 100 U/ml streptomycin; #10378016, Invitrogen) were used appended to the growth medium. All cells were incubated at 37 °C in a humidified atmosphere with 5% CO_2.

2.3. Cell transfection with miRNA mimics and luciferase reporter assay

Control microRNA (miRNA), *miR-433-3p* and *miR-433-5p* were procured commercially from GenePharma (Shanghai, China). The control miRNA mimics were used as external controls. Using a commercially available transfection reagent (Lipofectamine RNAiMAX Reagent; #13778100, Invitrogen Incorporation), cells were transfected with control miRNAs *miR-433-3p* and *miR-433-5p* (50 nM). Insertions of *SMAD2* and *ID-1* 3′-UTRs were made into a pGL vector (#E1751; Promega) respectively. These inserts contained putative binding sites for *miR-433-3p* or *miR-433-5p*. Six-well plates were seeded with cells and co-transfected with 100 pmol of miRNA mimics with 2 μg of luciferase reporter plasmid, and 200 ng of *Renilla* control reporter vector. Luciferase activity was measured 48 h post-transfection using a dual-luciferase reporter assay system (#E1910; Promega). Findings were normalized to *Renilla* luciferase activity. Id1 luciferase activity was analyzed as previously described [10].

2.4. Quantitative real-time RT-PCR (qRT-PCR)

Total cellular and tissue RNA was isolated using Trizol reagent (#15596026, Invitrogen incorporation). Expression of *miR-433* was evaluated using a commercially available Taqman MicroRNA kit (#4366596, Applied Biosystems, Foster City, USA). Real-time quantitative reverse

transcription PCR (qRT-PCR) was executed using the SYBR Green Master Mix (#A25741, Applied Biosystems). Expression studies were undertaken in triplicates and the average results were reported. Data were analyzed using the $2^{-\Delta\Delta CT}$ method and normalized to U6 small nuclear RNA. qRT-PCR was carried out using SYBR Green (#A25742, Invitrogen) to evaluate *SMAD2* expression. *GAPDH* levels were used as control for qRT-PCR analysis. Primers for *SMAD2* were as follows: sense, 5′-GCGGAATTCAACATGTCGTCCATCTTGCCATTC-3′; anti-sense, 5′−CCAGCTCGAGTTATGACATGCTTGAGCAACG-3′. Primers for *GAPDH* were as follows: sense, 5′-GAAGGTGAAGGTCGGAGTC-3′; anti-sense, 5′-GAAGATGGTGATGGGATTTC-3′.

2.5. Cell viability assay

Control miRNA or *miR-433* transfected cells (A549 or H23) were seeded in plates (96-well) at 200 cells per well in DMEM supplemented with 10% FBS for 0–4 days. Following incubation, cells were stained with 0.5 mg/ml of a commercial preparation of 3-(4,5-dimethylthiazol-2-yl)-2,5-diphenyltetrazoliumbromide (MTT) dye (#88417, Sigma, St Louis, USA) and incubated in darkness for 2 h at 37 °C. Subsequently, the culture medium was removed and formazan crystals were solubilized in dimethyl sulfoxide (#D8418, Sigma). Absorbance was measured at 570 nm. Experiments were undertaken in triplicate and reported as means with standard deviations.

2.6. Cell proliferation assay

A commercially procured Click-iT EDU assay kit (#E10415, Invitrogen incorporation) was used to perform the 5-Ethynyl-2′deoxyuridine (EDU) assay. Briefly, triplicates of 10^5 transfected cells were

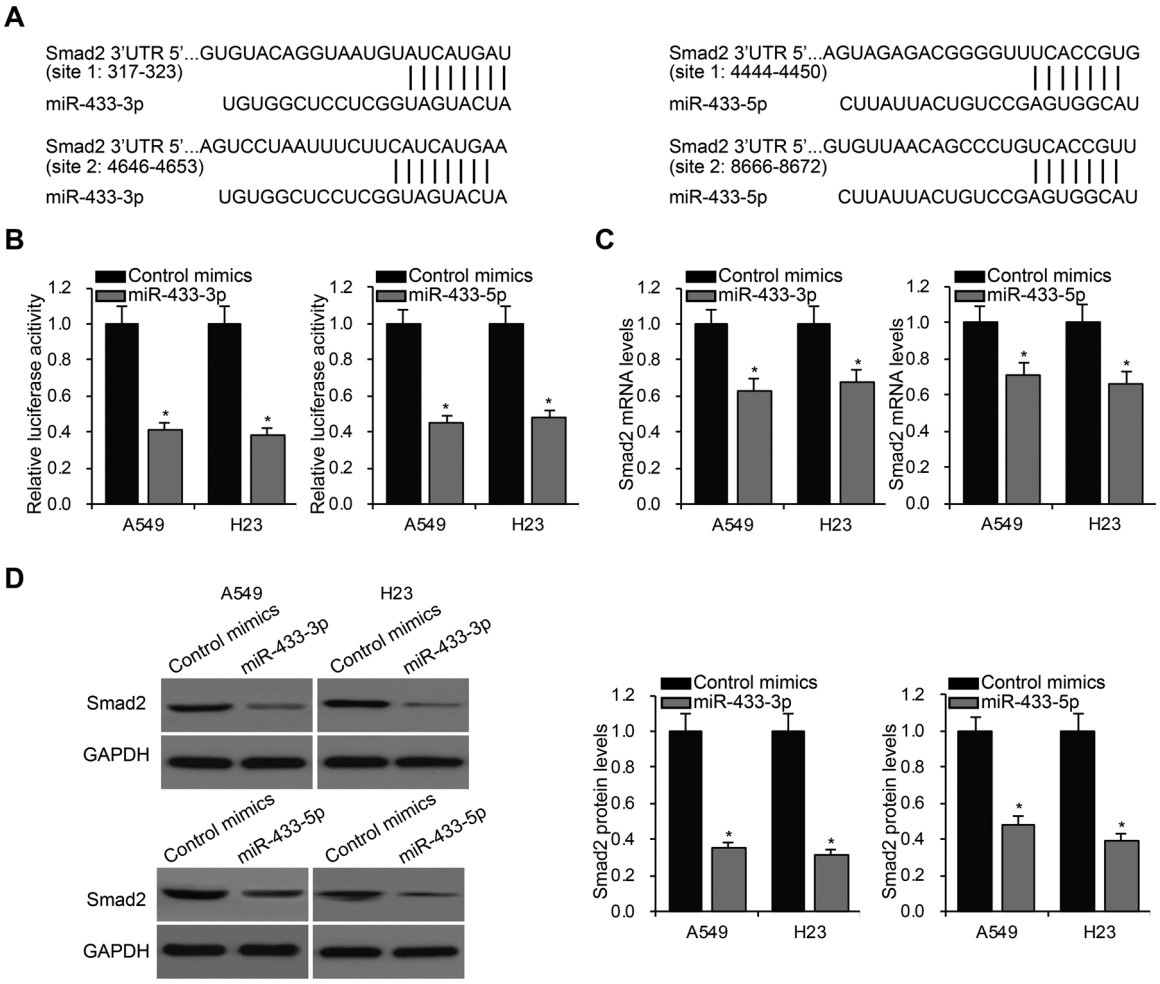

Fig. 4. *miR-433* directly targets Smad2. (A) Sequences of the potential *miR-433-3/5p* binding sites in Smad2 3′-UTRs. (B) Luciferase activity in A549 and H23 cells transfected with 3′-UTR luciferase reporter plasmid and miRNA mimic (control or miR-433). (C) qRT-PCR of *Smad2* mRNA expression in A549 and H23 cells transfected with miR-433 mimic or control miRNA mimic. (D)Western blot of Smad2 expression in A549 cells and H23 cells transfected with *miR-433* mimic or control miRNA mimic. Quantified density of Smad2 was shown. $^{*}P < 0.05$ vs. control mimics group.

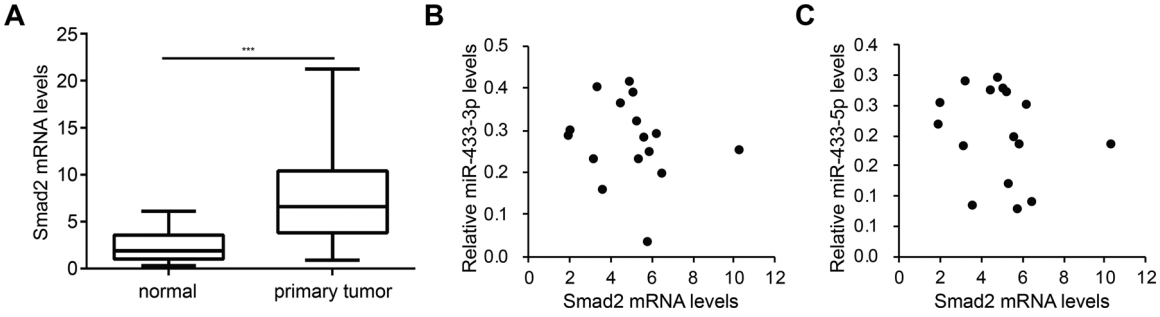

Fig. 5. Correlation between *miR-433* and *Smad2* in NSCLC. (A) The expression levels of *Smad2* mRNA were determined in primary NSCLC tissues and normal adjacent tissues by qRT-PCR. $^{***}P < 0.001$ vs. normal group. (B) Inverse correlation between *miR-433-3p* expression and *Smad2* mRNA expression determined by qRT-PCR assay of 50 NSCLC samples. $r = -0.551$, $P < 0.01$. (C) Inverse correlation between *miR-433-5p* expression and *Smad2* mRNA expression determined by qRT-PCR assay of 50 NSCLC samples. $r = -0.519$, $P < 0.01$.

seeded in four well chamber slides. The slides were incubated for 24 h and upon incubation, cells were exposed to EDU (20 mM) for another 4 h. All incubations were performed at 37 °C. Post incubation, cells were fixed, membranes were permeabilized and reactions were initiated with the Click-iT® cocktail for approximately 1 h. Hoechst 33,342 (5 μg/ml) was used as a nuclear counter stain.

2.7. Transwell invasion and migration analysis

Pre-coated Matrigel (1.5 mg/ml) transwell chambers of 8-μm pore size (#354480, BD Bioscience, San Jose, CA, USA) were used for cell invasion assays. Transfected cells (1×10^5 cells), re-suspended in serum-free medium were seeded in the upper chamber of the transwell. Non-Matrigel-coated inserts were used as experimental controls for cell migration analysis. The DMEM medium containing 10% FBS was supplemented into the lower chamber and the assembly was incubated for

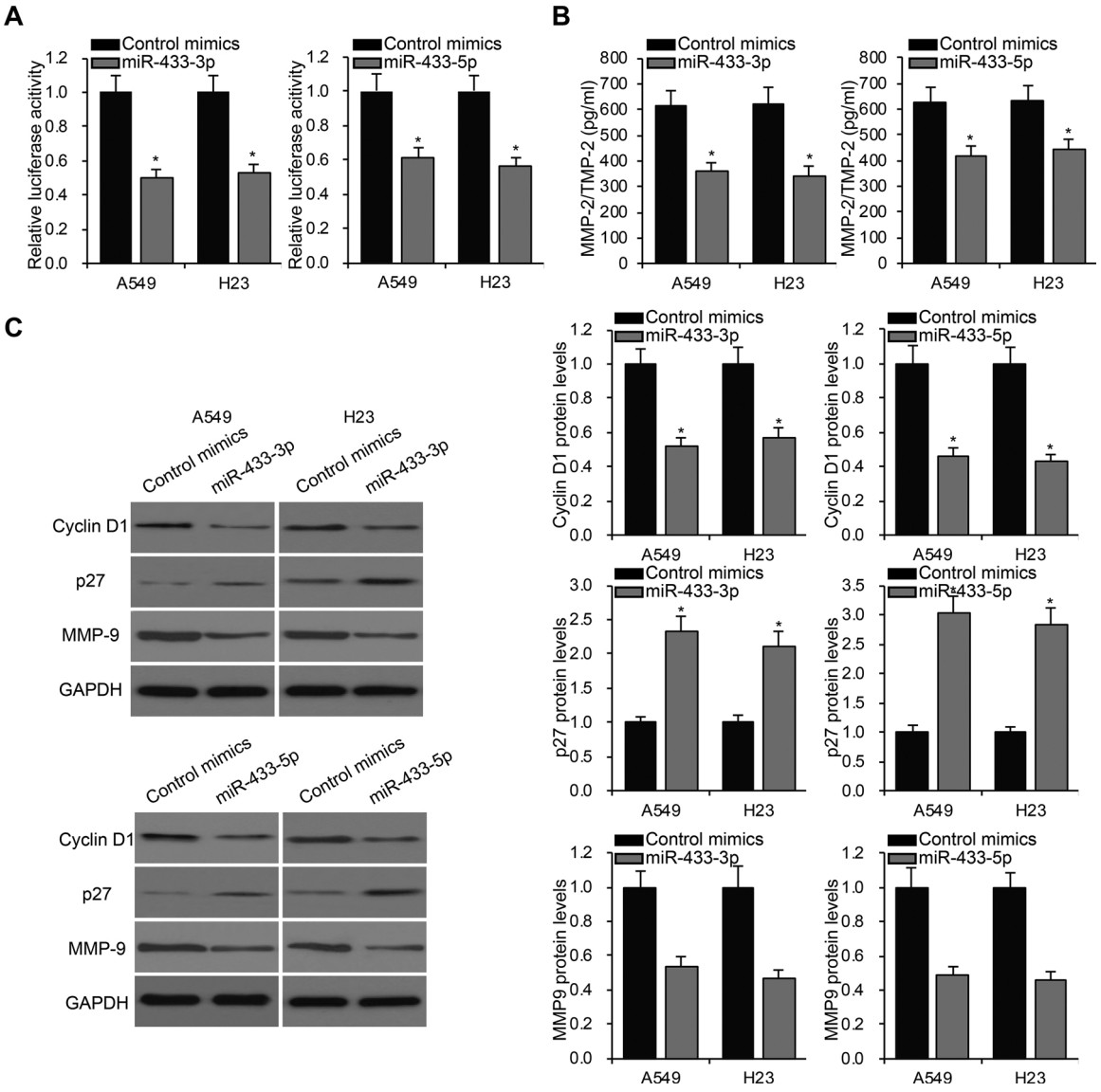

Fig. 6. *miR-433* regulates Smad signaling. (A) The ID1 luciferase activity in A549 cells and H23 cells transfected with *miR-433* mimic or control miRNA mimic. (B) The activity of MMP-2/TIMP-2 was measured in A549 cells and H23 cells transfected with miR-433 mimic or control miRNA mimic using ELISA. $^*P < 0.05$ vs. control mimics group. (C) Western blot of Cyclin D1, p27 and MMP-9 expression in A549 cells and H23 cells transfected with *miR-433* mimic or control miRNA mimic. Quantified density of each bind was shown. $^*P < 0.05$ vs. control mimics group.

24 h at 37 °C in 5% CO_2. Following incubation, cells were removed from the upper chamber by carefully cleaning the surface. The migrated and invaded cells were stained using crystal violet (0.1%) and imaged under a light microscope (with 100x magnification, # NSKT-100 V/R, Nikon, Tokyo, Japan). Using five pre-determined fields, the numbers of invasive and migratory cells were counted.

2.8. Western blot analysis

Cellular protein was extracted using the standard procedure using radioimmunoprecipitation assay (RIPA) buffer. Briefly, cells were incubated with ice-cold RIPA supplemented with a commercial preparation of a protease and phosphatase inhibitor cocktail (#PPC1010, Sigma). Upon estimation of the total protein concentration with Quick Start™ Bradford Protein Assay (#5000204, Bio-Rad, Hercules, USA), a fixed amount was separated on a 10% SDS-PAGE gel. The separated proteins were subsequently transferred to a nitrocellulose membrane through electro blotting. The protein-containing membranes were blocked, and probed for Smad2 (#sc-393312), Cyclin D1 (#sc-8396), p27 (#sc-1641) and MMP-9 (#sc-21733), overnight, using commercially-available antibodies (Santa Cruz Biotechnology). GAPDH (#sc-32233) was used as the loading control. The antibodies were incubated with a horse radish peroxidase (HRP)-conjugated secondary antibody (sc-2005), and developed using enhanced chemiluminescence (ECL) substrate (#sc-2048, Santa Cruz Biotechnology).

2.9. Assessment of MMP-2/TIMP-2 levels

Culture supernatants from cells transfected with control miRNA or *miR-433* were collected and assessed for levels of MMP-2/TIMP-2. The assessment was undertaken using a commercial Human MMP-2/TIMP-2 complex DuoSet enzyme linked immunosorbent assay (ELISA) from R& D Systems, Minneapolis, MN, USA (#DY1497).

2.10. Xenograft experiments

The animal experiments were approved by the Research Ethics Committee of the Second Affiliated Hospital of Harbin Medical

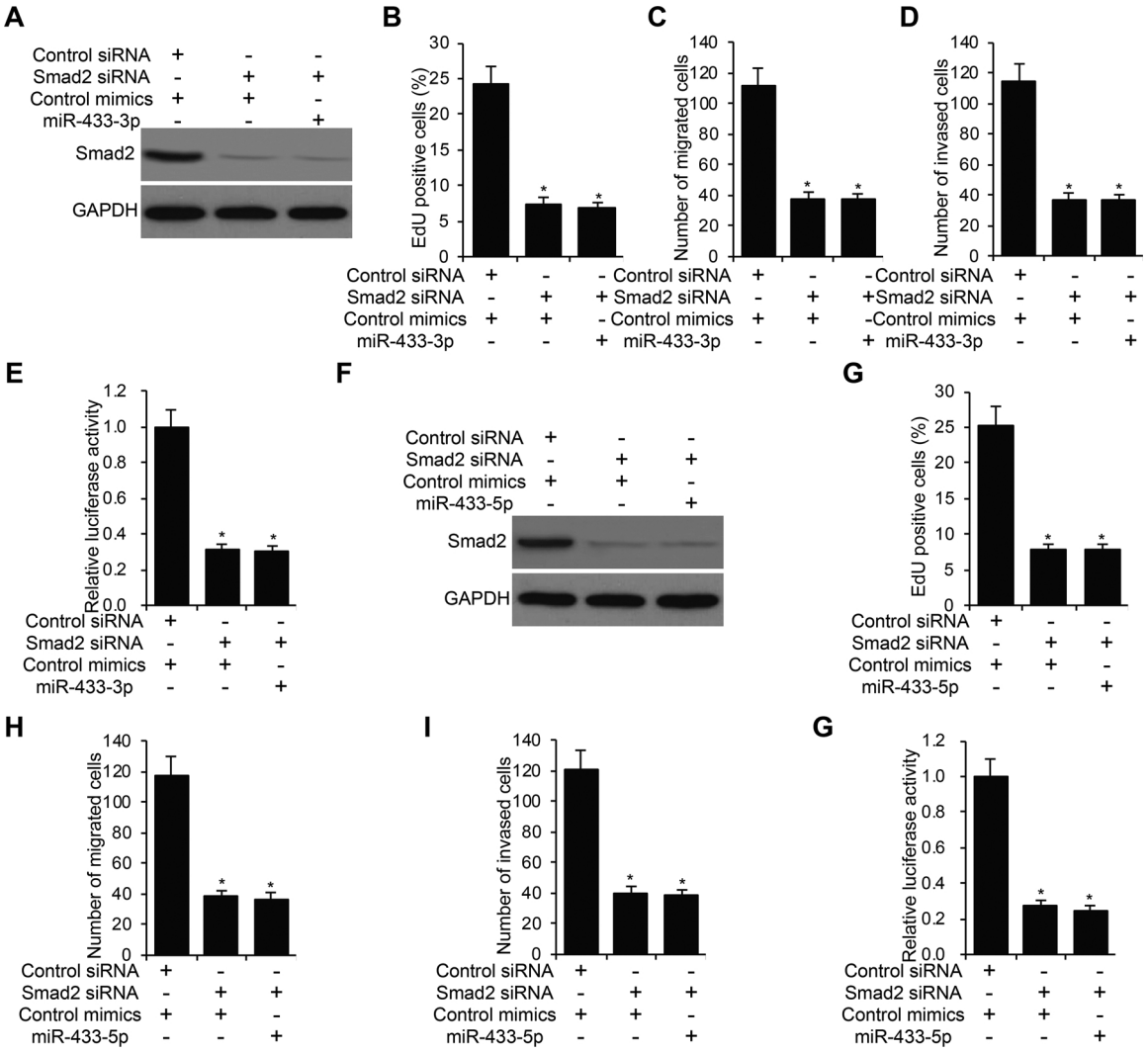

Fig. 7. *miR-433* regulates NSCLC cells through Smad2. (A) A549 cells were introduced Control siRNA + Control mimics, *Smad2* siRNA + Control mimics or *Smad2* siRNA + miR-433-3p. EdU (B), migration (C), invasion (D) and ID1 luciferase assays (E) were performed in (A). (F) Control siRNA + Control mimics, *Smad2* siRNA + Control mimics or *Smad2* siRNA + *miR-433-3p* were introduced to A549 cells. EdU (G), migration (H), invasion (I) and ID1 luciferase assays (J) were performed in (F).

University. Levntivirus-Control (LV-Control) mimics, LV-miR-433-3p- and LV-miR-433-5p-introduced A549 cells were established. Twenty nude BALBC/c mice were separated into four groups randomly. 200 µl A549 cell suspensions (1×10^7 cells) in PBS were subcutaneously injected into the right flanks of the nude BALBC/c mice to establish a xenograft NSCLC model. The mice were then raised in an isolated temperature controlled and pathogen-free environment. Sterilized food and autoclaved water were provided according to the experimental animal guidelines. After 25 days, all mice were sacrificed, and tumors were harvested, weighed and imaged.

2.11. Statistical analysis

The Student's *t*-test or one-way ANOVA was used to assess differences in means between groups. All experiments were performed in triplicate and the results were reported as mean ± standard deviation (SD). Statistically significant differences were considered only when *P-value* was < 0.05. A licensed version of SPSS software version 19.0 was used to analyze the data.

3. Results

3.1. miR-433 expression is dysregulated in NSCLC

miR-433 has reportedly been correlated with malignancy in a number of cancers. However, the association between *miR-433* and lung cancer has not been investigated. To study *miR-433* in NSCLC, we evaluated *miR-433-3p* and *miR-433-5p* expression in NSCLC tissues from 20 patients USING qRT-PCR. We found that *miR-433-3p* and *miR-433-5p* expression was down-regulated in lung tumor tissues in comparison to adjacent non-tumor lung tissues (Fig. 1A and 1B). These findings demonstrate that *miR-433* is downregulated in NSCLC.

3.2. miR-433 reduces NSCLC cell proliferation

To study the effect of *miR-433* in NSCLC development, selected NSCLC cell lines (A549, H23, H1869 and H1650) were transfected with control miRNA mimics or *miR-433*. Efficiency of transfection were confirmed using qRT-PCR which revealed significantly higher *miR-433-3p* and *miR-433-5p* expression in *miR-433* transfected cells than that in the control miRNA mimic-transfected cells (Fig. 2A and Supplemental Fig. 1A). Reduced cellular proliferation was observed in the miRNA

mimic transfected cells relative to the control mimic-transfected cells. Proliferation was assessed using the EdU assay and showed similar results across these cell lines (Fig. 2B and Supplemental Fig. 1B). Consistent with the above findings, the results of the MTT assay also corroborated the reduced cell proliferation phenotype in response to overexpression of *miR-433* in NSCLC cells *in vitro* (Fig. 2C and Supplemental Fig. 1C). Furthermore, the tumor xenograft experiments confirmed of inhibition of miR-433-3p and miR-433-5p in NSCLC cell proliferation (Fig. 2D). These findings indicate that *miR-433-3p* and *miR-433-5p* may reduce NSCLC cell proliferation.

3.3. miR-433 inhibits NSCLC migration and invasion

miR-433-mediated cellular migration and invasion was assessed using *in vitro* models. Ectopic expression of *miR-433-3p* and *miR-433-5p* significantly inhibited cell migration (Fig. 3A and Supplemental Fig. 2A). Simultaneously, we also observed a reduction in the number of invaded cells following *miR-433-3p* and *miR-433-5p* overexpression (Fig. 3B and Supplemental Fig. 2B). These results are suggestive of an anti-metastatic role of *miR-433-3p* and *miR-433-5p*.

3.4. miR-433 directly targets Smad2

Using a bioinformatics-based approach, we identified probable gene targets of *miR-433* using an miRNA target prediction database (TargetScan). We found that the oncogene Smad2, with multiple binding sites for both miR-433-3p and miR-433-5p, was a potential target (Fig. 4A). Upon construction of a luciferase reporter plasmid and transfection with control and *miR-433* mimics, we observed that Luciferase activity in A549 and H23 cells transfected with *Smad2* 3′UTR-encoding plasmid was significantly reduced by miR-433-3p and *miR-433-5p* (Fig. 4B). These observations were further supported by qRT-PCR and western blot analyses to confirm reduction in Smad2 mRNA and protein levels, resepectively. Moreover, we observed a significant reduction in the Smad2 expression profiles in the presence of *miR-433* mimics relative to the control miRNA mimics (Fig. 4C, 4D, Supplemental Fig. 3A and 3B).

3.5. Correlation between miR-433 and Smad2 in NSCLC

Tumor tissues which had dysregulated levels of *miR-433* were found to have significantly higher expression of *Smad2* in comparison to the paired adjacent controls. Moreover, *Smad2* expression was found to be inversely correlated with *miR-433-3p* ($r = -0.551$) and *miR-433-5p* ($r = -0.519$) expression (Fig. 5B). These results confirm *Smad2* as a target of miR-433-3p and *miR-433-5p* in NSCLC.

3.6. miR-433 regulates Smad signaling

Smad2 is a key protein in the Smad signaling pathway [3]. We investigated whether *miR-433-3p* and *miR-433-5p* regulate Smad signaling based on Id1 luciferase activity. Both *miR-433-3p* and *miR-433-5p* significantly decreased Id1 luciferase activity (Fig. 6A and Supplemental Fig. 4A). In addition, *miR-433-3p* and *miR-433-5p* also decreased the activity of MMP-2/TIMP-2 relative to the control group (Fig. 6B and Supplemental Fig. 4B). We next analyzed the expression of genes downstream of Smad (Cyclin D1, p27 and MMP9) [10]. As expected, the expression of Cyclin D1 and MMP9 was down-regulated and p27 was up-regulated by *miR-433-3p* and *miR-433-5p* in A549 and H23 cells.

To further investigate whether *miR-433* regulates Smad signaling through Smad2, we increased *miR-433-3p* expression in A549 cells with *Smad2* knockdown. Expression of Smad2 was examined after *Smad2* knockdown by western blot (Fig. 7A). These cells were subjected to EdU, migration, invasion and Smad luciferase assays. As shown in Figs. 7B-E, *miR-433-3p* failed to affect these processes in NSCLC cells after Smad2 knockdown. We next observed the same results for *miR-433-5p* (Fig. 7F to 7 G). Together, these results indicatethat *miR-433* regulates Smad signaling in NSCLC by targeting Smad2.

4. Discussion

Smads are intracellular signal mediators of the transforming growth factor-beta super family members. Activation of Smads through phosphorylation results in nuclear translocation of the protein thereby regulating the expression and repression of several genes. There are eight Smads present in vertebrates, of which Smad2/3 are activated through phosphorylation by TGF-β and activin receptors. TGF-β is a critical cytokine mediating several cellular processes and including cell proliferation, angiogenesis and metastases. Aberrations in the TGF-β signaling pathway have been linked to several diseases including multiple types of cancer. While it is well known that TGF-β processes its signal downstream through Smads, TGF-independent Smad modulation is a lesser-studied process. Our study assesses epigenetic modification of Smad using *microRNA-433* (*miR-433*), which has also been implicated in several cancers. However, its role in lung cancer has yet to be explored.

We first evaluated the levels of *miR-433* in treatment and surgery naïve patients. We found that the endogenous levels of *miR-433* were decreased in non-small cell lung carcinoma (NSCLC) patients. Our findings are consistent with other studies, reporting significantly reduced levels of *miR-433* in cancer cells and tissues of the breast [27] and lungs [16]. These studies exemplify the probable tumor suppressive role of *miR-433*, Cancer specific activities of microRNAs being explained by their identified targets, may be either oncogenic or tumor suppressive.

To further elaborate on the role of *miR-433* in non-small cell lung carcinoma, we overexpressed both *miR-433-3p* and *miR-433-5p* in NSCLC cell lines (A549 and H23). The overexpression of *miR-433* was associated with reduced cellular proliferation and reduced invasion. Loss of regulation of cell cycle is critical to maintaining a balance between cellular growth and apoptosis. As has been reported previously, TGF-β induces higher levels of cyclin D1 in breast cancer cells [6]. Cyclin D1, a regulatory subunit catalyzes the rate limiting step for cell transition from G1-S phase. Through molecular studies, Cyclin D1 has been identified as an important collaborative oncogene. Activation of cyclins is mediated through cyclin dependent kinases, regulated by phosphorylation and inhibited by kinase inhibitor proteins (KIPs). The over expression of P27 and the consequent downregulation of Cyclin D1 is probably due to upregulation of KIPs, which is concurrent with findings in other cancers [5,6,9]. The reduction in the endogenous levels of Cyclin D1 may inhibit Cyclin D1 and p27 complex formation, thereby reducing migration. As has been reported previously, in Cyclin D1 -/- which display deficiencies in migration, the phenotype was rescued by the introduction of *P27KIP1* small interfering RNA [15].

Recent studies have also identified the role of inhibitor of differentiation (Id) proteins, particularly Id1, in the promotion of invasion, angiogenesis and metastasis. Increased expression of Id-1 was found to enhance proliferation and metastasis through PI3k/Akt mediated Wnt signaling pathway in breast cancer cell lines [14]. Our study substantiates that *miR-433* binds directly to Id-1, thereby inhibiting its functions in cellular proliferation and invasion, thereby inhibiting important tumorigenic pathways in NSCLC.

Malignancy and relapse are major hurdles in solid tumors such as NSCLC. Large cohort studies have identified MMP-2/TIMP-2 [4] and MMP-9 [7,13] as prognostic markers for malignancy and relapse, respectively. MMP-2/TIMP-2 [23] and MMP-9 have both been shown to be regulated by Id-1. Whilst MMP-2/TIMP2 expression is regulated through the NF-κB pathway, the invasive function of Id-1 is attributed to MMP-9 [20]. Thus, the repression of Id-1 in the presence of *miR-433* may lead to inhibition of invasion and reduce relapses *in vivo*.

Whilst our study addresses the role of *miR-433* in progression of NSCLC, studies elucidating the yin and yang of *miR-433* are far and few.

It would help to understand what factors de-regulate the expression of *miR-433*, whether these factors constitutive or induced, whether they are host-derived or environmental, and whether they are disease and stage specific or ubiquitous. To this end, future experiments are required.

5. Conclusions

The current study strengthens the therapeutic and prognostic potential of miRNAs, which, although having been explored *in vitro,* remain elusive as a therapy for the lack of reliable delivery and targeting abilities. Furthermore, this study also highlights the significance of *miR-433* in regulating crucial metabolic pathways which are essential for maintaining cellular homeostasis. While the findings of the study are presented in the context of NSCLC, these may be extrapolated and evaluated for other diseases with similar clinicopathological characteristics.

Author contribution

JL performed the experiments, collected the data and wrote the manuscript, MC analyzed the data, BY designed the manuscript and analyzed the data.

Declaration of Competing Interest

The authors declared no conflicts of interest in this study.

Acknowledgement

None.

Appendix A. Supplementary data

Supplementary material related to this article can be found, in the online version, at doi:https://doi.org/10.1016/j.prp.2019.152591.

References

[1] T. Berghmans, M. Paesmans, J.P. Sculier, Prognostic factors in stage III non-small cell lung cancer: a review of conventional, metabolic and new biological variables, Ther. Adv. Med. Oncol. 3 (2011) 127–138.
[2] F. Bray, J. Ferlay, I. Soerjomataram, R.L. Siegel, L.A. Torre, A. Jemal, Global cancer statistics 2018: GLOBOCAN estimates of incidence and mortality worldwide for 36 cancers in 185 countries, CA Cancer J. Clin. 68 (2018) 394–424.
[3] K.A. Brown, J.A. Pietenpol, H.L. Moses, A tale of two proteins: differential roles and regulation of Smad2 and Smad3 in TGF-beta signaling, J. Cell. Biochem. 101 (2007) 9–33.
[4] C. Cao, N. Xu, X. Zheng, W. Zhang, T. Lai, Z. Deng, X. Huang, Elevated expression of MMP-2 and TIMP-2 cooperatively correlates with risk of lung cancer, Oncotarget 8 (2017) 80560–80567.
[5] A.V. Carvalhal, I. Marcelino, M.J. Carrondo, Metabolic changes during cell growth inhibition by p27 overexpression, Appl. Microbiol. Biotechnol. 63 (2003) 164–173.
[6] M. Dai, A.A. Al-Odaini, N. Fils-Aime, M.A. Villatoro, J. Guo, A. Arakelian, S.A. Rabbani, S. Ali, J.J. Lebrun, Cyclin D1 cooperates with p21 to regulate TGFbeta-mediated breast cancer cell migration and tumor local invasion, Breast Cancer Res. 15 (2013) R49.
[7] M.K. El-Badrawy, A.M. Yousef, D. Shaalan, A.Z. Elsamanoudy, Matrix metalloproteinase-9 expression in lung cancer patients and its relation to serum mmp-9 activity, pathologic type, and prognosis, J. Bronchology Interv. Pulmonol. 21 (2014) 327–334.
[8] P.O. Eser, P.A. Janne, TGFbeta pathway inhibition in the treatment of non-small cell lung cancer, Pharmacol. Ther. 184 (2018) 112–130.
[9] W.M. Flanagan, J.J. Wolf, P. Olson, D. Grant, K.Y. Lin, R.W. Wagner, M.D. Matteucci, A cytosine analog that confers enhanced potency to antisense oligonucleotides, Proc. Natl. Acad. Sci. U. S. A. 96 (1999) 3513–3518.
[10] M. Guo, Z. Jiang, X. Zhang, D. Lu, A.D. Ha, J. Sun, W. Du, Z. Wu, L. Hu, K. Khadarian, J. Shen, Z. Lin, miR-656 inhibits glioma tumorigenesis through repression of BMPR1A, Carcinogenesis 35 (2014) 1698–1706.
[11] Y. He, Z. Zhou, W.L. Hofstetter, Y. Zhou, W. Hu, C. Guo, L. Wang, W. Guo, A. Pataer, A.M. Correa, Y. Lu, J. Wang, L. Diao, L.A. Byers, I.I. Wistuba, J.A. Roth, S.G. Swisher, J.V. Heymach, B. Fang, Aberrant expression of proteins involved in signal transduction and DNA repair pathways in lung cancer and their association with clinical parameters, PLoS One 7 (2012) e31087.
[12] H.S. Jeon, J. Jen, TGF-beta signaling and the role of inhibitory Smads in non-small cell lung cancer, J. Thorac. Oncol. 5 (2010) 417–419.
[13] C.Y. Lee, H.S. Shim, S. Lee, J.G. Lee, D.J. Kim, K.Y. Chung, Prognostic effect of matrix metalloproteinase-9 in patients with resected Non small cell lung cancer, J. Cardiothorac. Surg. 10 (2015) 44.
[14] J.Y. Lee, M.B. Kang, S.H. Jang, T. Qian, H.J. Kim, C.H. Kim, Y. Kim, G. Kong, Id-1 activates Akt-mediated Wnt signaling and p27(Kip1) phosphorylation through PTEN inhibition, Oncogene 28 (2009) 824–831.
[15] Z. Li, X. Jiao, C. Wang, X. Ju, Y. Lu, L. Yuan, M.P. Lisanti, S. Katiyar, R.G. Pestell, Cyclin D1 induction of cellular migration requires p27(KIP1), Cancer Res. 66 (2006) 9986–9994.
[16] N. Liu, Z. Liu, W. Zhang, Y. Li, J. Cao, H. Yang, X. Li, MicroRNA433 reduces cell proliferation and invasion in nonsmall cell lung cancer via directly targeting E2F transcription factor 3, Mol. Med. Rep. 18 (2018) 1155–1164.
[17] F. Louafi, R.T. Martinez-Nunez, T. Sanchez-Elsner, MicroRNA-155 targets SMAD2 and modulates the response of macrophages to transforming growth factor-{beta}, J. Biol. Chem. 285 (2010) 41328–41336.
[18] Z. Lu, Y. Tang, J. Luo, S. Zhang, X. Zhou, L. Fu, Advances in targeting the transforming growth factor beta1 signaling pathway in lung cancer radiotherapy, Oncol. Lett. 14 (2017) 5681–5687.
[19] H. Luo, H. Zhang, Z. Zhang, X. Zhang, B. Ning, J. Guo, N. Nie, B. Liu, X. Wu, Down-regulated miR-9 and miR-433 in human gastric carcinoma, J. Exp. Clin. Cancer Res. 28 (2009) 82.
[20] M. Nieborowska-Skorska, G. Hoser, L. Rink, M. Malecki, P. Kossev, M.A. Wasik, T. Skorski, Id1 transcription inhibitor-matrix metalloproteinase 9 axis enhances invasiveness of the breakpoint cluster region/abelson tyrosine kinase-transformed leukemia cells, Cancer Res. 66 (2006) 4108–4116.
[21] I. Shi, N. Hashemi Sadraei, Z.H. Duan, T. Shi, Aberrant signaling pathways in squamous cell lung carcinoma, Cancer Inform. 10 (2011) 273–285.
[22] E. Shtivelman, T. Hensing, G.R. Simon, P.A. Dennis, G.A. Otterson, R. Bueno, R. Salgia, Molecular pathways and therapeutic targets in lung cancer, Oncotarget 5 (2014) 1392–1433.
[23] Y. Su, L. Gao, L. Teng, Y. Wang, J. Cui, S. Peng, S. Fu, Id1 enhances human ovarian cancer endothelial progenitor cell angiogenesis via PI3K/Akt and NF-kappaB/MMP-2 signaling pathways, J. Transl. Med. 11 (2013) 132.
[24] R.L. Toonkel, A.C. Borczuk, C.A. Powell, Tgf-beta signaling pathway in lung adenocarcinoma invasion, J. Thorac. Oncol. 5 (2010) 153–157.
[25] R.N. Wang, J. Green, Z. Wang, Y. Deng, M. Qiao, M. Peabody, Q. Zhang, J. Ye, Z. Yan, S. Denduluri, O. Idowu, M. Li, C. Shen, A. Hu, R.C. Haydon, R. Kang, J. Mok, M.J. Lee, H.L. Luu, L.L. Shi, Bone Morphogenetic Protein (BMP) signaling in development and human diseases, Genes Dis. 1 (2014) 87–105.
[26] Z. Yang, H. Tsuchiya, Y. Zhang, M.E. Hartnett, L. Wang, MicroRNA-433 inhibits liver cancer cell migration by repressing the protein expression and function of cAMP response element-binding protein, J. Biol. Chem. 288 (2013) 28893–28899.
[27] T. Zhang, K. Jiang, X. Zhu, G. Zhao, H. Wu, G. Deng, C. Qiu, miR-433 inhibits breast cancer cell growth via the MAPK signaling pathway by targeting Rap1a, Int. J. Biol. Sci. 14 (2018) 622–632.